A Computational Study of Ligand Interactions with Hafnium and Zirconium Metal Complexes in the Liquid−Liquid Extraction Process[§]

G. Gopi Krishna, R. Sudarshan Reddy, P. Raghunath, K. Bhanuprakash,* M. Lakshmi Kantam, and B. M. Choudary*

Inorganic Chemistry Division, Indian Institute of Chemical Technology, Hyderabad-500 007, India

Received: August 20, 2003; In Final Form: December 8, 2003

In this paper we present a computational study of ligand interactions with hafnium and zirconium metal complexes which occur in the liquid−liquid extraction of these metals from their aqueous solutions. Separation of Hf and Zr has been a challenge in liquid−liquid extraction technologies and the existing methodologies, namely the MIBK (methyl isobutyl ketone) process, are used to extract hafnium into the organic phase while on the contrary the TBP (tributyl phosphate) process is used to extract Zr into the organic phase. Understanding the actual interactions taking place, including an estimate of the binding energies and conformations of the guest−host system of the metal complexes and the solvents, would help us to design better and safer extractants. Recent studies in the literature have shown that the quantum chemical based DFT methods have proven to be good tools for such types of studies. Thus in this work we have carried out high-level DFT studies using the hybrid B3LYP/Lanl2dz and BLYP/TZP (with the relativistic corrections) on tetravalent Hf and Zr metal complexes interacting with neutral ligands and compared the results to the experimental observations. These studies show that at the molecular level it is the Hf complex that has larger interaction energy with the ligands, thus indicating that in the mixture of Hf and Zr complexes in solutions which are not complicated by aggregation and polymerization, Hf would be extracted preferably into the organic solvent, in agreement with the experimental observation. We conclude from this study that primary interaction energies (gas-phase stabilization) are sufficient to significantly discriminate Hf and Zr complexes and thus can be used to explain Hf and Zr separation.

Introduction

The design of new ligands for efficient separation of cations in general and metal cations in particular is very important and challenging, keeping in view the present day emphasis on decreasing the environmental problems present in the existing extraction technologies.[1] One of the most widely used technologies for these metal separations is the liquid−liquid extraction of the cations from their aqueous solutions with an organic solvent. From the viewpoint of designing new extractants or improving the existing ones, understanding the exact nature of guest−host interactions including the binding (interaction) energies and conformational features of these metals binding to the extractants would be very useful. In this regard theoretical studies using quantum chemical principles can play a major role for the quantitative predictions of the stability and geometrical parameters and has been used with success in the lanthanide and other metal series by many workers.[2−5] Wipff and co-workers have studied the interactions of M^{3+} lanthanide cations with amides, pyridines, and phosphoryl ligands using both HF and DFT methods.[2] They concluded, based on the interaction energies calculated, that the $O{=}PPh_3$ ligand is a better extractant. In another study from the same group, they observed the importance of the counterions and stoichiometry for the binding between the ligand and the metal.[3] Studies on alkali and alkaline earth metal cations interacting with π electron systems using the quantum chemical principles have revealed π−metal interactions to be substantial.[4]

In the second and third transition series, the separation of Hf and Zr presents a challenging task due to the near similar chemical and physical properties of the two metals. There are three widely used processes for the separation of these metals out of which two of them, namely the MIBK and TBP processes, are based on liquid−liquid extraction (Scheme 1).[6] The MIBK process, which is named after the extractant methyl isobutyl ketone, is the process in which the thiocyanic complexes of Hf and Zr formed in an acid media get separated with a factor of 7 with the Hf complex getting enriched in the organic layer and the Zr complex in the aqueous layer.[6] In this process reported by Fischer et al., first the thiocyanic acid is distributed between the organic phase (MIBK) and the aqueous phase before the metal oxychlorides are added.[7] After the addition of the metals the aqueous phase now contains numerous complexes of Zr/Hf formed with OH^-, SCN^-, and water, of which it is only those complexes with high SCN content that are extracted. On the basis of the experiments carried out on the partition coefficients, they observed that as the metal concentration was increased for a given quantity of the thiocyanic acid, then the increase in nonextractable complexes with low SCN content would increase and this leads to a decrease in partition coefficient as seen in their graphs. They also observed that at lower metal concentrations the partition coefficient tends toward a constant value. This led them to the inference that the metal would be largely present as a single species and these species themselves would be identical. They concluded that the

[§] IICT Communication No. 030805.

* Author to whom the correspondence has to be addressed. E-mail: bhanu2505@yahoo.co.in.

10.1021/jp036477p CCC: $27.50
Published on Web 04/17/2004

SCHEME 1

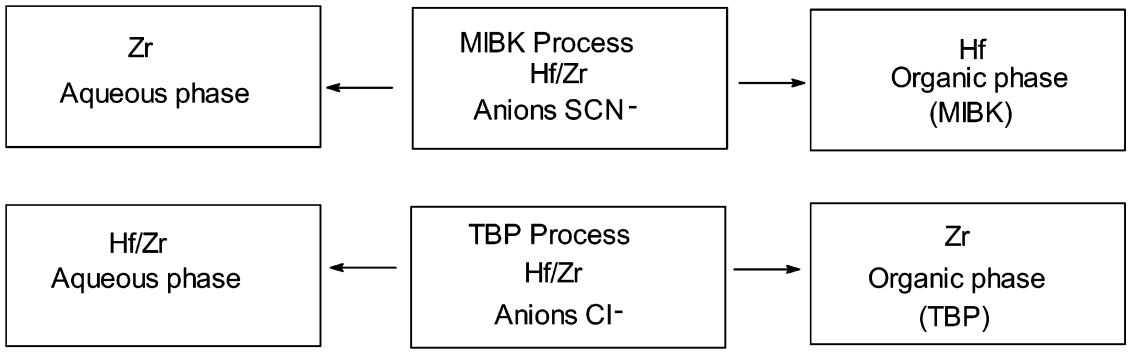

preferential extraction of Hf over Zr is either due to the extractable species of metal being more stable or having higher individual partition coefficients. This method has the advantages of being cost-effective and having simultaneous production of pure Hf and Zr. The disadvantages in this process are that the MIBK has miscibility with water and the waste streams contain toxic substances such as ammonium and cyanide salts. The organic solvent itself is highly volatile and explosive. On the other hand, in the TBP process, which is also named after the extractant, tributyl phosphate, it is Zr that gets enriched in the organic solvent. Here the metals are extracted as chloride complexes, in a fairly high acid media that prevents hydrolysis and polymerization.[8] The separation factor here is around ten. This method suffers from the disadvantages that it is twice the cost of the MIBK process and specific only to obtaining pure Zr, while the mixtures in the aqueous layers are wasted. To improve the TBP process, studies have been carried out using the Cyanex series of extractants.[9,10] But it still remains as a challenge to develop a cost-effective and environmentally friendly technology to separate these two metals.

To develop a new extractant, say like a macrocyclic ring, which is known to be very ion specific, the exact interactions going on in the two processes must be understood. Earlier experiments have addressed the efficiency of extraction varying a number of parameters such as the concentration of acids, the role of metal concentrations, the common ion, etc., but to the best of our knowledge the interaction energies and geometry of these metal complexes interacting with the extractant have not been studied.[6−10] The general extraction picture is that in the aqueous solution a series of species such as $MX^{4-y}{}_y \cdot ZH_2O$ is formed, where X represents the anions. Some of the species are probably in polymerized form.[6] While experimental evidence points out the fact that the metal complexes in higher acid concentrations and an excess of anions in both process are extracted as a single species (no polymerization) and as neutral MX_4 complexes, studies have also indicated that they are extracted as disolvated molecules, i.e., $MX_4 \cdot$2solvent molecules.[9−11]

Thus with the general view of understanding the interactions of these metal complexes with the solvents and with the more specific aim of developing an efficient extractant, we have taken up this theoretical study. Our aim is to obtain the quantitative picture of the interaction energies (primary interactions), which will give us an insight into the nature of Zr/Hf interacting with TBP/MIBK. While our intention is not to explain the exact extraction sequence through our methods here, some questions we propose to ask and answer are what are the molecular level interactions (gas phase) of Zr and Hf complexes with the P═O group and the the C═O groups, and what conformations do these complexes adopt with the ligands. For this we define some energy terms, which are useful for understanding the difference

CHART 1

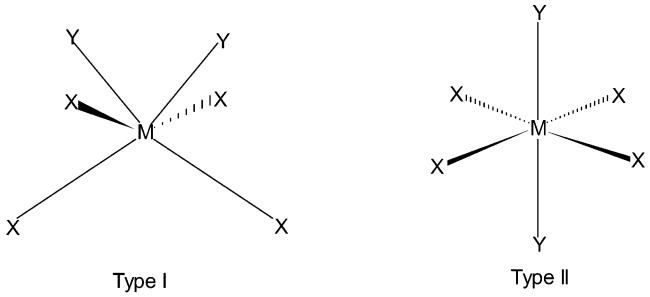

[Y=ligand, M=Hf/Zr, X=anions]

in the stability of Hf and Zr complexes. We carry out our studies using the ab initio Hartree−Fock method and the density functional method (DFT). For the DFT method we used both Gaussian 98(G98) software, which uses Gaussian orbitals, and also the Amsterdam Density Functional package (ADF), which is based on the Slater-type orbitals.[12,13]

Computational Methods

Recent literature reports have indicated that the Lanl2dz basis in conjunction with either the HF or the DFT methods are well-suited for studies involving solvent extraction of metals.[2−5] In addition these have also been found to perform well for the studies involving Zr and Hf.[14,15] Thus this basis set was our choice for both the HF and Becke's hybrid DFT method (B3LYP).[16] The Lan2dz option places double-ζ functions on the valence shells of the heavier atoms while the inner shells are represented by electron core potentials (ECP), but for the first-row atoms the Lan2dz basis is essentially the D95 basis with no ECPs.[17] Minimizations have been carried out based on the experimental evidence that the metals are tetravalent and disolvated. As we are interested in the relative energy differences we have also assumed disolvation in the case of water as ligand. In all our calculations the MIBK has been replaced with acetone and TBP with trimethyl phosphate (TMP) for computational convenience and no restraints have been placed in any geometry optimizations.

There are two possible orientations (broadly) for the two solvent molecules (ligands) to interact with the complex. Both are shown in Chart 1, wherein one of them has both the solvent molecules interacting from the same direction (cis) and the other from opposite directions (trans or the axial interactions), which we call type I and type II, respectively. Experimental studies in the solid state indicate that type I structures are formed, which has also been confirmed by larger stabilities obtained in DFT studies involving $ZrCl_4$ and formaldehyde.[14,18] We consider mainly type I structures, and for comparison type II structures

CHART 2

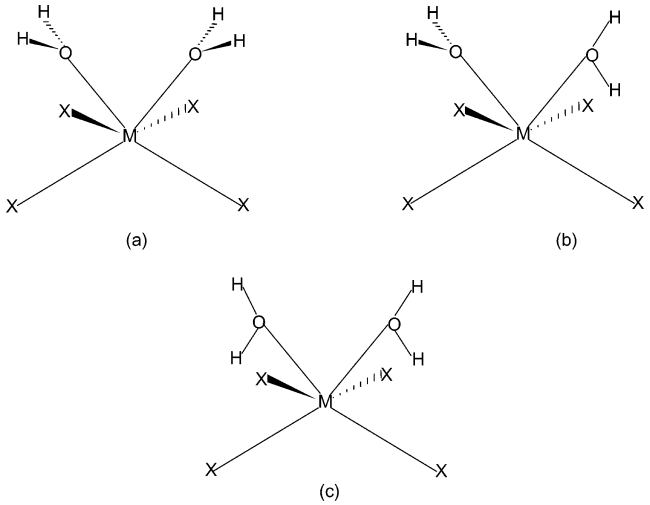

are also calculated here. Chart 2 shows three possible conformations of type I structures, **a**, **b**, and **c**. In **a**, the solvent molecules are parallel, **b** is the perpendicular arrangement, while **c** is a side on arrangement. We find that with water **a** has the lowest energy, while for bulkier solvents **c** becomes the most stable conformation. The starting geometry for both Hf and Zr complexes is the same and only the lowest energy complex obtained for each metal has been reported in the paper. The stabilization energy of the tetravalent metal complex, MX_4, with the disolvent is defined as

$$\Delta E(\mathrm{M-Y}) = E(\mathrm{MX_4 \cdot 2Y}) - E(\mathrm{MX_4}) - 2.0E(\mathrm{Y}) \quad (1a)$$

where $E(MX_4 \cdot 2Y)$ is the total energy of the $MX_4 \cdot 2$solvent molecules complex, while $E(MX_4)$ is the total energy of the in situ formed MX_4 fully minimized in the absence of the ligand molecules. Here it should be kept in mind that the minimized structure corresponding to $E(MX_4)$ will not necessarily correspond to the gas-phase global minima. $E(Y)$ is the total energy of the fully minimized ligand molecule without the metal complex. Thus the stabilization energy obtained here would be equal to the interaction energy of MX_4 with the 2 ligands, in which the geometry relaxation energy of the isolated fragments and the interaction between the ligands have also been included.

We also define another energy term for each solvent, $\Delta\Delta E$, which would help us to evaluate the metal that has a larger stabilization in the solvent (with a particular ligand)

$$\Delta\Delta E = \Delta E(\mathrm{Hf-Y}) - \Delta E(\mathrm{Zr-Y}) \quad (2)$$

Here $\Delta E(Hf-Y)$ and $\Delta E(Zr-Y)$ have been calculated by using eq 1a. For example, if the above-mentioned energy was to be zero, it would mean both Hf and Zr have equal affinity or interaction energy to the ligand, or in other words the solvent would stabilize both metal complexes equally. If the above $\Delta\Delta E$ was to have a negative sign then Hf would be preferentially stabilized in the solvent.

To supplement the studies carried out with DFT B3LYP/Lanl2dz (will be referred to as the B3LYP method) Gaussian methods, we also calculated the geometries and energies of the molecules using the BLYP hybrid method and the relativistic Hamiltonian ZORA (will be referred to as BLYP in the rest of the text).[19−20] The basis set used for this study is the Slater-type orbitals, TZP, which have been optimized for the relativistic calculations.[13,21] Here too the ECP were used with the TZP only

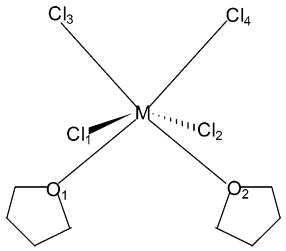

Figure 1. Structure of MCl_4 complexed with 2THF molecules, where M=Hf/Zr. The detailed experimental and calculated bond lengths and angles are shown in Table 1.

on the valence shells. The interaction energy has been calculated by using eq 1b (vide infra). The interaction energy calculated this way does not take into account the geometry relaxation of the fragments and also the interaction energies of the ligand molecules within themselves including H-bonding. The basic equation is given below.

$$\Delta E(\mathrm{M-Y}) = E^{\mathrm{SP}}(\mathrm{MX_4 \cdot 2Y}) - E^{\mathrm{SP}}(\mathrm{MX_4}) - E^{\mathrm{SP}}(\mathrm{2Y}) \quad (1b)$$

SP indicates a single point at the minimized geometry of $E(MX_4 \cdot 2Y)$. $E^{SP}(MX_4)$ and $E^{SP}(2Y)$ are the single point runs in the absence of ligand and complex molecules, respectively, at the minimized geometry of $E^{SP}(MX_4 \cdot 2Y)$. The reason for using eq 1b in this method is to carry out the energy partition analysis for estimating the components of the energy contributing to the binding (an option available in ADF only).[13] Here we also estimate the basis set superposition error (BSSE) that may arise due to the basis sets for the interactions.[22]

Finally here we define another energy term that would help us to understand the metal complexes loss or gain in energy in replacing the interacting water with the solvent molecules.

$$\Delta E_s = \Delta E(\mathrm{M}) - \Delta E'(\mathrm{M}) \quad (3)$$

Here $\Delta E(M)$ is the ΔE in water and $\Delta E'(M)$ is the ΔE in solvent. In this case if for any metal the sign of ΔE_s obtained is negative then this implies that the metal would be stabilized more with the solvent ligand than with H_2O.

Results and Discussions

$MCl_4 \cdot 2THF$. Since the main aim of this work is to understand the differences in the interactions and geometries of identical Hf and Zr complexes interacting with neutral ligands, first we judge the quality of the basis set and the HF/DFT methods for reproducing such geometries of Hf/Zr complexes involving weak interactions. For this we searched the literature for experimentally determined structures of both Hf and Zr identical complexes interacting with the same neutral ligands and we were able to obtain only such type of crystallographic structure from the CSD and in this structure $ZrCl_4/HfCl_4$ interact with THF(tetrahydrofuran), which is shown in Figure 1, and geometrical parameters are given in Table 1.[23,24] Experimental Hf/Zr−Cl bond lengths are of two types, one close to the metal and the other slightly longer, thus the Hf−Cl bond lengths are 2.363/2.376 and 2.400/2.388 Å while the Zr−Cl bond lengths are 2.397/2.389 and 2.425/2.422 Å, respectively. B3LYP calculations using C_s symmetry reproduce these bond lengths very well. The predicted Hf−Cl distances are 2.416 and 2.473 Å, respectively, which differ from the solid-state geometries by 0.06 to 0.08 Å. In the case of Zr−Cl the deviation is also small and these are between 0.04 and 0.06 Å. For the weaker interactions, bond lengths of the oxygen of THF interacting with the metal, the values

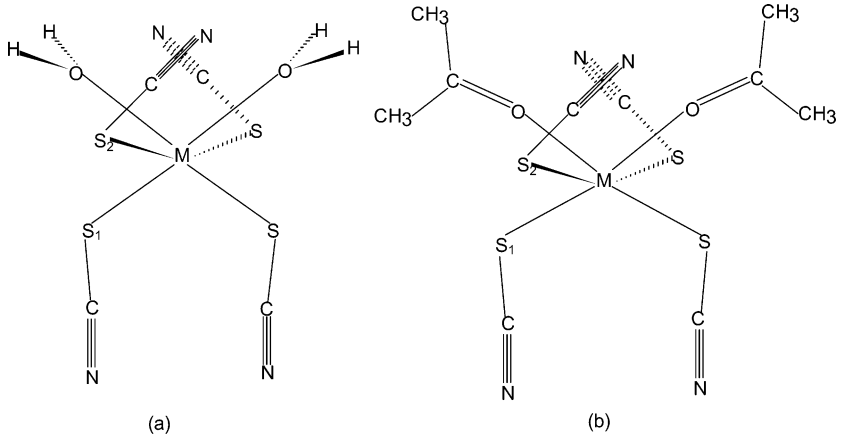

Figure 2. Minimized geometries (C_s symmetry) of $M(SCN)_4$ interacting with 2 H_2O (a) and 2 acetones (b) molecules. Selected bond lengths shown in Table 2(a).

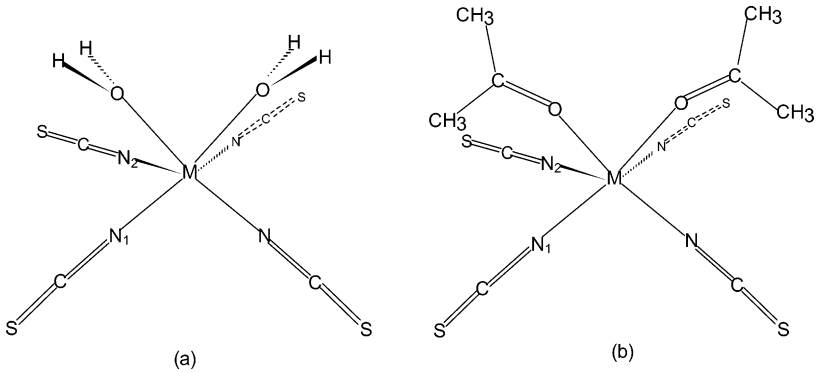

Figure 3. Minimized geometries (C_s symmetry) of $M(NCS)_4$ interacting with 2 H_2O (a) and 2 acetones (b) molecules. Selected bond lengths shown in Table 2(b).

TABLE 1: The Comparison of Crystal Structures Obtained from References 22 and 23 and Those Calculated by Various Methods in This Study for MCl_4·2THF (where M = Hf, Zr)[a]

	Hf (Zr)			
bond	HF	B3LYP	BLYP	cryst struct.
M−Cl_1	2.499 (2.516)	2.473 (2.493)	2.463 (2.486)	2.388 (2.425)
M−Cl_2	2.499 (2.516)	2.473 (2.493)	2.463 (2.486)	2.400 (2.422)
M−Cl_3	2.446 (2.458)	2.416 (2.434)	2.399 (2.424)	2.363 (2.397)
M−Cl_4	2.446 (2.458)	2.416 (2.434)	2.399 (2.424)	2.376 (2.389)
M−O_1	2.206 (2.246)	2.229 (2.277)	2.334 (2.382)	2.196 (2.237)
M−O_2	2.206 (2.246)	2.229 (2.277)	2.334 (2.382)	2.200 (2.229)
O_1MCl_3	85.7 (83.7)	84.9 (84.2)	84.2 (82.8)	86.0 (87.2)
O_2MCl_4	85.7 (83.7)	84.9 (84.2)	84.2 (82.8)	86.1 (86.6)
Cl_1MCl_2	166.9 (164.9)	164.2 (162.5)	163.4 (162.1)	171.0 (170.4)
Cl_3MCl_4	99.6 (100.2)	99.3 (99.8)	80.4 (100.5)	98.4 (98.5)
O_1MO_2	84.4 (84.2)	83.1 (83.1)	80.4 (80.2)	81.6 (81.2)

[a] Bond lengths are in angstroms and bond angles are in degrees. Data for Zr are given in parentheses.

obtained are 2.196 and 2.2 Å which are comparable to the calculated 2.229 Å. Again in the case of Zr−O distances the experimental geometries are 2.237 and 2.229 Å which are comparable to the B3LYP distances of 2.277 Å. The deviations are small.

In the same table values obtained with HF and BLYP are reported. BLYP predicts slightly longer Hf−O and Zr−O bond lengths. But for M−Cl the bond lengths are much closer to the experimental value. Interestingly the HF method predicts M−O bonds in very good agreement with the experimental data, unlike the M−Cl bonds, which are slightly deviated. Overall the agreement of the experimental structure with the calculated ones in all cases is very good. The relative difference in Zr and Hf is brought about by all the methods in a similar fashion as in the experimental structure, with the corresponding bonds involving Zr always longer.

Extraction in the MIBK Process. The question that arises now is whether the complex is thiocyanate (S-bonded) or isothiocyanate (N-bonded), i.e., SCN^- or NCS^-.[25] Recent DFT calculations on the coordination and hydrogen bonding properties of copper thiocyanate complexes indicate that N-bonding is preferred to the S-bonding in the gas phase but as the H-bonding with solvent molecules was taken into account in the S-bonded structures the relative total energies start narrowing down.[26] Thus the possibility of formation of the N-bonded metal complex (Hf/Zr) case is reduced. In addition in this process the thiocyanate ions form first and it can be assumed that in the aqueous media the N end is stabilized leaving the S end free for bonding.

We considered both SCN and NCS anions here and show as added proof that based on the interaction energies, the SCN complexes have more probability of formation. The geometries of the minimized structures are shown in Figure 2a for SCN complexes interacting with H_2O and Figure 2b for the corresponding acetone complexes. Similarly parts a and b of Figure 3 depict the NCS complexes interacting with water and acetone. Only the selected bond lengths obtained by the three methods are shown in Table 2 for clarity. It can be seen in Table 2 that in all cases the Zr−O and Zr−X bond length is longer than the Hf−O and Hf−X bond lengths, respectively, in agreement with what we observed in the MX_4·2THF experimental and theoretically determined structures (shown in Table 1). Within each metal's case the bond lengths of the M−O bond, when O is ketonic, is smaller than the M−O bond lengths obtained in the water case. Thus in the SCN case, the Hf−O bond length in

TABLE 2: Selected Bond Lengths (in Å) Obtained for $M(SCN)_4 \cdot 2$ligands, $M(NCS)_4 \cdot 2$ligands, and $M(Cl)_4 \cdot 2$ligands of Type I Structure in C_s Symmetry by Various Methods in This Study[a]

		Hf (Zr)		
solvent	bonds	HF	B3LYP	BLYP
		(a) $M(SCN)_4 \cdot 2$ligands		
water	$M-S_1$	2.542 (2.558)	2.522 (2.547)	2.529 (2.559)
	$M-S_2$	2.649 (2.672)	2.643 (2.669)	2.631 (2.659)
	M−O	2.204 (2.241)	2.189 (2.231)	2.257 (2.304)
acetone	$M-S_1$	2.585 (2.601)	2.555 (2.577)	2.562 (2.584)
	$M-S_2$	2.685 (2.707)	2.652 (2.678)	2.632 (2.663)
	M−O	2.057 (2.092)	2.068 (2.115)	2.134 (2.175)
		(b) $M(NCS)_4 \cdot 2$ligands		
water	$M-N_1$	2.061 (2.081)	2.047 (2.073)	2.054 (2.090)
	$M-N_2$	2.111 (2.135)	2.100 (2.128)	2.109 (2.145)
	M−O	2.265 (2.307)	2.269 (2.313)	2.391 (2.427)
acetone	M−N	2.088 (2.108)	2.066 (2.092)	2.083 (2.109)
	M−N	2.115 (2.156)	2.095 (2.122)	2.119 (2.156)
	M−O	2.164 (2.205)	2.205 (2.255)	2.281 (2.328)
		(c) $M(Cl)_4 \cdot 2$ligands		
water	$M-Cl_1$	2.406 (2.423)	2.387 (2.409)	2.376 (2.406)
	$M-Cl_2$	2.480 (2.494)	2.459 (2.477)	2.438 (2.469)
	M−O	2.243 (2.284)	2.248 (2.294)	2.388 (2.426)
tmp	$M-Cl_1$	2.534 (2.549)	2.502 (2.518)	2.479 (2.504)
	$M-Cl_2$	2.507 (2.521)	2.459 (2.474)	2.423 (2.445)
	M−O	2.045 (2.081)	2.086 (2.134)	2.215(2.264)

[a] Data for Zr are given in parentheses.

TABLE 3: Stabilization Energies ΔE(eq 1a) and the difference in ΔE, $\Delta\Delta E$(eq 2), for $MX_4 \cdot 2$ligands Calculated by Using B3LYP and HF (in kcal/mol)[a]

		HF		B3LYP	
X	ligands	ΔE	$\Delta\Delta E$	ΔE	$\Delta\Delta E$
SCN^-	water	−87.3 (−84.3)	−3.2	−77.6 (−73.0)	−4.6
	acetone	−109.8 (−104.7)	−5.1	−81.6 (−75.3)	−6.3
NCS^-	water	−59.9 (−56.9)	−3.0	−53.2 (−50.3)	−2.9
	acetone	−66.3 (−63.1)	−3.2	−49.3 (−46.0)	−3.0
Cl^-	water	−67.2 (−64.3)	−2.9	−58.4 (−54.6)	−3.8
	TMP	−111.3 (−105.1)	−6.2	−73.1 (−66.3)	−6.8

[a] Data for Zr are given in parentheses (for the definition of ΔE and $\Delta\Delta$E see the text).

the acetone solvent is 2.068 Å and in water it is 2.189 Å, while in the case of Zr−O, for acetones the bond length is 2.115 Å and in water it is 2.231 Å (as obtained in B3LYP). The geometries of the isolated ligands namely H_2O and acetone are not reported, but since here we are discussing the geometry at the complex, it would be of interest to know the changes in the bond length of the interacting groups. The C═O bond length of the isolated ketone is 1.249 Å and it lengthens to 1.277 Å in the case of binding with Hf and to 1.276 Å in Zr (all in B3LYP method). The change is around 0.028 Å. In the studies on the lanthanide series, the interactions of a ketone group with MCl_3, the M−O distance variation from Eu to La is 2.277 to 2.387 Å, much larger than the variation of bond length of around 0.04 Å in Hf−O and Zr−O.[3]

The stabilization energies are tabulated in Table 3 obtained for the HF and B3LYP methodologies, while in Table 4 the results of the BLYP method along with energy partitioning is shown. In the case of the SCN complex with H_2O as the ligand, the ΔE value obtained in the B3LYP method is −77.6 kcal/mol for Hf and −73.0 kcal/mol in the case of Zr. The HF values are not very different, yielding −87.3 and −84.3 kcal/mol, respectively. In either case the Hf is having a larger stabilization energy, which is also seen by using the BLYP method (using eq 1b) in Table 4 (−69.7 and −66.8 kcal/mol). On an average the difference in stabilization, $\Delta\Delta E$, of the Hf complex over that of the Zr complex predicted by all three methods is around 2.9 to 4.6 kcal/mol when interacting with H_2O. The small differences arising between B3LYP and BLYP methods should be due to the different definitions of ΔE(eq 1a and 1b). It should be understood that the complex with SCN is being formed in situ in aqueous solutions, and Hf and Zr would compete with each other to form this stable complex. The more stable complex would be the one that is extracted first to the organic phase. Thus the stabilization energies indicate that the Hf complex (more exothermic) is more stable than the Zr complex in the aqueous solutions.

The stabilization of the complex in the organic media is now important, and the calculated stabilization energies in Tables 3 and 4 indicate that the Hf complex in the organic solvent has a stabilization energy of −81.6 kcal/mol when compared to −75.3 kcal/mol in the Zr case. That means a clear stabilization of the Hf complex in the acetone solvent also but now by 6.3 kcal/mol. In the calculations with HF and BLYP the energies predicted are similar and the stabilization energies are −5.1 kcal/mol in HF and −5.8 kcal/mol in the BLYP case. ΔE_s of the Hf complex, or the gain, is as much as −12.7 kcal/mol in replacing the H_2O ligands with the organic ligands, while Zr gains only −9.8 kcal/mol (Table 4). Thus in competition between the Hf and Zr thiocyanate complexe formation in situ and extraction into the organic solvent, the free energy of Hf is always more and hence it would move preferentially to the organic media. The extra exothermic energy for $Hf(SCN)_4$ over $Zr(SCN)_4$ right from its formation to its extraction into the organic solvent can be written as the sum of (using only the gas-phase energies) $\Delta\Delta E(H_2O) + \Delta\Delta E(Me_2C{=}O) + \Delta E_s$(difference of H_2O and acetone), which turns out to be 11.6 kcal/mol for Hf over that of Zr (in BLYP). Thus the extraction of Hf should always be more than Zr, or rather larger partition coefficient should be obtained. This is in agreement with the observation by Fischer et al. in the studies involving individual metals that they find the Hf partition coefficients are always larger than those for Zr.[7]

We next turn to case of NCS anions, which are given in the same tables. Here the total energy of the corresponding isomers when compared to the SCN complex is lower, i.e., the $M(SCN)_4 \cdot 2H_2O$ has a higher total energy than $M(NCS)_4 \cdot 2H_2O$ (not shown in tables). This is always the case for both water and the solvent and also for both metals. But if the stabilization energies are taken into account it can be seen that the SCN complex always has a larger interaction energy with the solvent and that too is around 20−30 kcal/mol (Tables 3 and 4). This is also irrespective of the metal and solvent. This gives us a more realistic picture, and as these complexes are being formed in situ, the driving force would be the larger enthalpy of formation. The larger stabilization in the SCN case arises due to the nonbonded interactions of the ligand and the anions. This is reflected in the energy components in Table 4, which we shall discuss in detail later. On the basis of this we can say that the SCN complex is formed preferentially. Nevertheless even if the NCS complex was to be formed also, the stabilization energies again are in favor of Hf. Thus the interaction with water is exothermic by about −53.2 kcal/mol when compared to −50.3 kcal/mol for the Zr (B3LYP). This gives additional stabilization of −2.9 kcal/mol for the Hf, while in the organic solvent the stabilization in favor of Hf is −3.0 kcal/mol. The values obtained by BLYP are not different, −2.6 and −3.8 kcal/mol, respectively. The extra exothermic energy (vide supra) in the NCS case would be −7.6 kcal/mol for the $Hf(SCN)_4$ over $Zr(SCN)_4$.

TABLE 4: The Energy Partition Analysis (kcal/mol), Including BSSE Along with ΔE(eq 1b), $\Delta\Delta E$(eq 2), and ΔE_s(eq 3) for $MX_4 \cdot 2$ligands of Type I Structures Obtained in This Study at the BLYP Level[a]

X	ligand	XC	CE	KE	EE	BSSE	ΔE	$\Delta\Delta E$	ΔE_s
SCN^-	water	−112.3 (−101.1)	−162.2 (−186.7)	333.9 (333.2)	−132.1 (−114.7)	2.9 (2.4)	−69.7 (−66.8)	−2.9	−12.7 (−9.8)
	acetone	−115.9 (−100.3)	−135.4 (−152.2)	303.6 (291.8)	−137.9 (−118.6)	3.3 (2.7)	−82.4 (−76.6)	−5.8	
NCS^-	water	−57.9 (−48.6)	−86.6 (−84.6)	176.2 (157.0)	−63.4 (−52.8)	1.5 (1.2)	−30.3 (−27.7)	−2.6	−21.2 (−20.0)
	acetone	−81.3 (−69.6)	−139.4 (−135.5)	257.5 (231.8)	−90.3 (−76.0)	2.0 (1.6)	−51.5 (−47.7)	−3.8	
Cl^-	water	−68.6 (−60.8)	−121.9 (−138.4)	242.2 (241.0)	−91.4 (−78.9)	1.8 (1.5)	−37.9 (−35.6)	−2.3	−33.0 (−28.7)
	TMP	−115.1 (−100.6)	−146.7 (−156.4)	312.7 (297.6)	−124.4 (−107.0)	2.6 (2.1)	−70.9 (−64.3)	−6.6	

[a] Data for Zr are given in parentheses; XC = exchange and correlation functional; CE = Coulombic (steric + orbital) interaction; KE = kinetic energy; EE = electrostatic energy; BSSE = basis set superposition error correction (for the definition of ΔE, $\Delta\Delta E$, ΔE_s see the text).

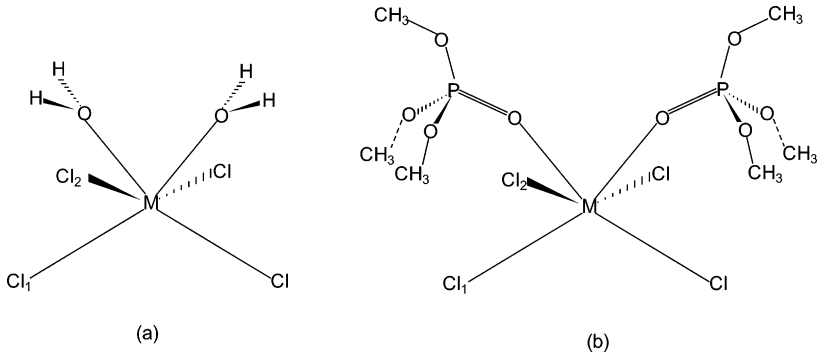

Figure 4. Minimized geometries of MCl_4 interacting with 2 H_2O (a) and 2 TMP (b) molecules (C_s). Selected bond lengths are shown in Table 2(c).

Extraction in the TBP Process. Here we shall assume that the metal exists as a tetrachloride, which would be the case in high acid concentrations where also the metal complexes would remain as single species (not dimeric or polymeric).[8−10] Here too disolvation occurs as shown by Distin and co-workers, who also studied in detail the effect of various concentrations of the acid and metals.[9] The geometries are shown in Figure 4 and tabulated in Table 2 while stabilization energies are tabulated for this set in Tables 3 and 4. The M−O distances in general for the TMP ligand interactions are shorter than those in SCN/NCS complexes. The change in the P═O bond length upon complexation is 0.008 Å (the uncomplexed P═O bond length is 1.579 Å while it is 1.587 Å for the Hf complex and 1.586 Å for the Zr complex). In the case of interaction energies tabulated in Tables 3 and 4, the first and the foremost thing which is observed is that the ΔE in the case of MCl_4 interacting with the ligand is much smaller for Hf and Zr when compared to the $M(SCN)_4$ interaction with ligands. The difference is much larger with H_2O, with a stability around 30 kcal/mol larger in SCN complexes. This probably is also the reason that in the MIBK process, the complex is present as a single species, but in the TBP process unless a larger number of Cl anions are present hydrolysis followed by polymerization takes place. This also indicates that in aqueous solutions if SCN and Cl ions were present, the SCN complexes of Hf and Zr would be preferably formed. The stabilization energies, ΔE, though not as large as in the earlier cases, still indicate that the Hf has a larger stabilization. The $\Delta\Delta E$ stabilizations (B3LYP) are around −3.8 kcal/mol in water and around −6.8 kcal/mol in TMP. Thus the $\Delta\Delta E$ values are larger than those obtained in SCN or NCS complexes. The agreement obtained by the HF or BLYP method is good. Again in line with our arguments for the SCN/NCS the stabilization of the Hf complex in both phases being faster, the extraction of the Hf complex would be faster. The ΔE_s for each of these metals is very high, −33kcal/mol for Hf and −28.7 kcal/mol for Zr, but the difference is around 4.3 kcal/mol again in favor of Hf. The extra exothermic energy for Hf over Zr complexes is 13.2 kcal/mol, about 2 kcal/mol larger than in the SCN complexes. Thus the calculations point out that the Hf complex is more favored in the organic phase as in the case of the MIBK process. This has a very good agreement with the recent work of Distin et al., who carried out the extraction studies using cyanex 923 (P═O ligand) at various acidities, various volumes of the extractants, and various concentrations of the metals.[9,10] It can be seen that with low metal concentration in high acid solutions, where the hydrolysis, aggregation, and polymerization can be assumed to be minimal, the Hf metal is extracted at a higher percentage into the organic solvent when the solvent is not in excess. Thus at 4 M of HCl, and when the metal concentrations are only around 0.002 M, the extracted Hf is around 85% and Zr at the same conditions is around 65%. The case with a slight increase in the metal concentrations is similar; but at much higher concentrations of the metal, like 0.05 M, the other factors such as polymerization and hydrolysis dictate the extraction. Here too when the acid concentration is very high the extraction starts becoming equal for both metals. These experiments have been carried out with individual metals separately and not as mixtures.[9,10]

Analysis of Energy Components. To understand the actual reason Hf seems to be more acidic than Zr toward these ligands (even though both cations have the same radius and charge), we analyzed the energy components obtained in the BLYP method using ADF and these are shown in Table 4. The BSSE for Hf and Zr turned out to be nearly the same and addition of this does not change the trend. Electrostatic energy is always larger with the organic ligand, for any given metal, than in H_2O, while between Hf and Zr the electrostatic energy of Hf is always larger. Electrostatic energy obtained for the SCN complex is the maximum. Coulombic energy is larger in Zr for SCN and Cl ions, while for NCS, they are larger in Hf. The exchange correlation energy is always larger for Hf and between H_2O and the ligand, it is larger for the ligand. From the values it seems that the larger electrostatic energy and larger exchange correlation energy obtained for Hf play a major part in the larger stability. The charges calculated by Mulliken's population analysis are shown in Table 5 and this indicates a larger positive charge on Zr all the time. Within the ligands the charge on the individual metal slightly increases from H_2O to (Me_2C═O), but

TABLE 5: Mulliken Charges Obtained for Type I Structures in C_s Symmetry at the BLYP Level[a]

X	ligand	M	X_1	X_2	O	dipole moment (debye)
S	water	1.02 (1.16)	−0.03 (−0.06)	−0.04 (−0.07)	−0.59 (−0.62)	7.2 (6.7)
	acetone	1.05 (1.19)	−0.08 (−0.10)	−0.06 (−0.09)	−0.60 (−0.63)	11.7 (10.0)
	−	0.82 (0.95)	0.03 (−0.01)	−0.004 (−0.04)	−	1.11 (1.32)
N	water	1.88 (2.08)	−0.39 (−0.43)	−0.43 (−0.47)	−0.60 (−0.62)	5.6 (5.3)
	acetone	1.89 (2.10)	−0.37 (−0.42)	−0.38 (−0.42)	−0.57 (−0.60)	10.1 (9.8)
	−	1.729 (1.84)	−0.38 (−0.43)	−0.44 (−0.48)	−	1.79 (1.72)
Cl	water	1.36 (1.53)	−0.43 (−0.46)	−0.43 (−0.46)	−0.60 (−0.62)	4.8 (4.8)
	TMP	1.52 (1.66)	−0.45 (−0.46)	−0.49 (0.52)	−0.83 (−0.85)	8.8 (8.4)
	- -	1.23 (1.36)	−0.34 (−0.37)	−0.342 (−0.37)	−	1.49 (1.47)

[a] Data for Zr are given in parentheses.

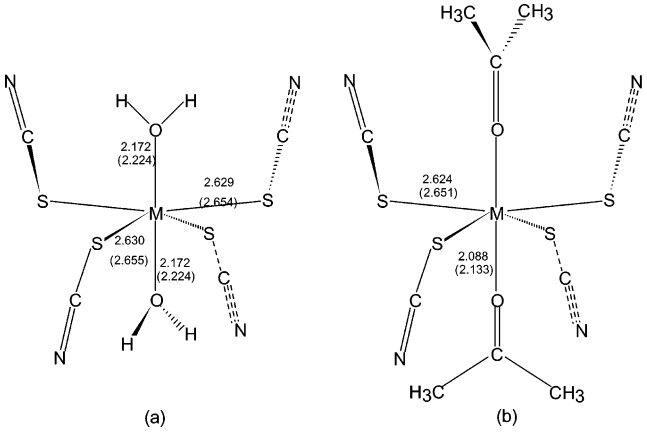

Figure 5. Minimized geometries of $M(SCN)_4$ interacting with 2 water (C_2 symmetry) (a) and 2 acetone (D_2 symmetry) (b) molecules. M=Hf/Zr, Zr bond lengths are given in parentheses.

for H_2O to TMP the charge transfer is much higher. Except for the case of TMP in all other cases the charges on O do not vary much. When compared to the charges on the bare metal complex (without the ligands), it can be seen that substantial charge transfer occurs from metal to the solvent, indicating the dominance of the electrostatic energy component. The large dipole moments support this.

Type II Structures and Higher Coordination. To compare the axial interactions (trans) of the ligands, interacting with the complex, with that of the cis type of interactions (type I), we have carried out computations on all three types of anions with the ligands using only the BLYP methodology. The minimized geometries are shown in Figures 5−7, where the bond lengths are also indicated. In general the anions NCS^- prefer a planar type of arrangement (C_{2v}), where as for SCN^- it tends to be nonplanar (D_2) in the complex. In the case of MCl_4 the planar C_s arrangement is preferred. The M−O bond lengths, in all these cases, are smaller than corresponding ones in the type I system. This is irrespective of the ligand.

The stabilization energies are shown in Table 6. The general trend is that larger ΔE are obtained here when compared to type I systems and this is reflected in $\Delta\Delta E$ also. Thus for SCN^- as the anions, the ΔE is as much as −105.3 kcal/mol for Hf and −93.9 kcal/mol for Zr, which is about 30 kcal/mol larger than the values for the type I systems. It is the same case with acetone as the ligand, where −107.8 and −97.4 kcal/mol have been obtained for Hf and Zr, respectively, which is again −20 k.cal/mol more stabilized than the type I systems. The $\Delta\Delta E$ in H_2O is −13.7 kcal/mol and in acetone it is −10.4 kcal/mol. In the case of Cl^- anions also the average increase is again around 20 kcal/mol, indicating that the type II systems show larger stabilization. The extra exothermic energy, defined earlier, here is as much as one-half times larger than in the type I case. The charge analysis is shown in Table 7, where it can be seen that the overall increase in the ΔE compare to the type I systems is largely due to electrostatic energies (larger charges).

The possibility of neutral higher coordination, i.e., 8 for the metal complexes interacting with solvents, is not ruled out, while our assumption of 6-coordination is based on experimental evidence. The possibility exists more so for anions such as Cl which are small when compared to SCN^-. Thus the 8-coordinated neutral species would also be extracted into the organic solvent, but would lose the water molecules if any before it enters the organic phase, which is based on the experimental studies with IR where the H_2O-coordinated complex was not detected in the organic solvent.[27] On the other hand more than two bulky solvent molecules interacting with the tetravalent complex are not possible due to steric hindrance. Hence all such coordinations exist only in the aqueous phase, which should then convert to 6-coordinated in the organic phase. Here we focus our study only on the chloride complexes with higher coordination number and use the BLYP method for estimating the interaction energies. We minimized a structure with 4 H_2O molecules interacting with the metal complex and also $2H_2O$ + 2TMP (hydrophobic one side) molecules interacting with the complex. This is shown in Figure 8. It will be of interest to

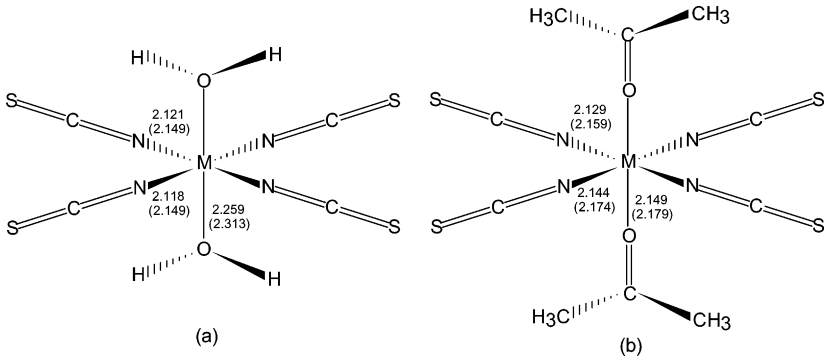

Figure 6. Minimized geometries (C_{2v}) of $M(NCS)_4$ interacting with 2 water (a) and 2 acetone (b) molecules. M=Hf/Zr, Zr bond lengths are given in parentheses.

TABLE 6: The Energy Partition Analysis (kcal/mol), Including BSSE Along with ΔE(eq 1b), $\Delta\Delta E$(eq 2), and ΔE_s(eq 3), for MX_4·ligands of Type II Structures Obtained in This Study at the BLYP Level[a]

X	ligand	XC	CE	KE	EE	BSSE	ΔE	$\Delta\Delta E$	ΔE_s
SCN^-	water	−148.9 (−129.0)	−238.4 (−243.8)	441.3 (417.1)	−159.3 (−138.2)	3.2 (2.7)	−102.1 (−91.2)	−10.9	−2.3 (−3.5)
	acetone	−122.7 (−102.3)	−147.9 (−167.7)	304.9 (294.6)	−142.0 (−122.0)	3.4 (2.7)	−104.4 (−94.7)	−9.7	
NCS^-	water	−69.3 (−56.7)	−132.6 (−117.6)	232.0 (196.2)	−87.5 (−72.8)	1.6 (1.1)	−55.9 (−49.7)	−6.2	−12.5 (−11.5)
	acetone	−90.2 (−78.4)	−175.4 (−174.3)	287.4 (270.3)	−92.6 (−80.6)	2.4 (1.8)	−68.4 (−61.2)	−7.2	
Cl^-	water	−72.5 (−63.0)	−117.9 (−149.6)	223.7 (240.0)	−93.8 (−81.9)	2.0 (1.6)	−58.5 (−53.5)	−5.0	−35.2 (−32.2)
	TMP	−125.7 (−106.9)	−224.9 (−242.0)	394.9 (381.4)	−140.9 (−120.5)	2.9 (2.4)	−93.7 (−85.7)	−8.0	

[a] Data for Zr are given in parentheses; XC = exchange and correlation functional; CE = Coulombic (steric + orbital) interaction; KE = kinetic energy; EE = electrostatic energy; BSSE = basis set superposition error correction (for the definition of ΔE, $\Delta\Delta E$, ΔE_s see the text).

TABLE 7: Mulliken Charges Obtained for Type II Structures at the BLYP Level[a]

X	ligand	M	X_1	X_2	O	dipole moment (debye)
S	water	1.11 (1.25)	−0.03 (−0.06)	−0.03 (−0.06)	−0.61 (−0.64)	0.0 (0.0)
	acetone	1.12 (1.27)	−0.08 (−0.11)	−0.08 (−0.11)	−0.60 (−0.63)	0.0 (0.0)
	−	0.86 (0.986)	0.02 (−0.02)	0.02 (−0.02)	−	0.0 (0.0)
N	water	1.83 (1.99)	−0.39 (−0.42)	−0.39 (−0.42)	−0.55 (−0.60)	0.0 (0.0)
	acetone	1.87 (2.08)	−0.37 (−0.41)	−0.37 (−0.41)	−0.56 (−0.61)	0.0 (0.0)
	−	1.62 (1.69)	−0.37 (−0.40)	−0.37 (−0.40)	−	0.0 (0.0)
Cl	water	1.39 (1.55)	−0.41 (−0.44)	−0.41 (−0.44)	−0.55 (−0.59)	0.0 (0.0)
	TMP	1.53 (1.67)	−0.49 (−0.51)	−0.49 (−0.51)	−0.85 (−0.88)	0.5 (0.8)
	−	1.26 (1.35)	−0.31 (−0.34)	−0.32 (−0.34)	−	0.1 (0.3)

[a] Data for Zr are given in parentheses.

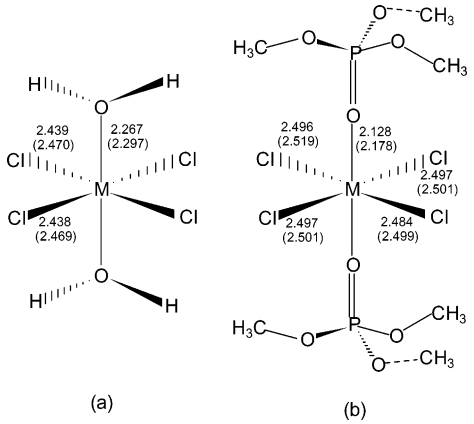

Figure 7. Minimized geometries of $M(Cl)_4$ interacting with 2 water (C_{2V} symmetry) (a) and 2 TMP(C_S symmetry) (b) molecules. M=Hf/Zr, Zr bond lengths are given in parentheses.

compare the geometries of the 6-coordinated complexes with those of the 8-coordinated complex. The M−Cl bond lengths are slightly elongated in the 8-coordinated species (Figure 8a), 2.509/2.513 Å, compared to the 6-coordinated species of 2.406/2.480 Å. Similar is the case of Zr−Cl bonds, where now the bond lengths of 6-coordinated species 2.494/2.423 Å have changed to 2.532/2.530 Å. This elongation is not much when the TMP ligands are interacting (Figure 8b) for 2 Cl molecules, but for the other 2 Cl molecules, the bond length of 2.534 (2.569) Å of Hf−Cl (Zr−Cl) becomes 2.662 (2.689) Å. The M−O bond lengths have elongated substantially when 6-coordinated species become 8-coordinated. In the case of $2H_2O$ + 2TMP interacting with the complex (Figure 8b), the M−O bond length of the $2H_2O$ is much larger, indicating more electrostatic interactions and fewer orbital interactions. The values are 2.549 (2.568) Å for Hf−O (Zr−O) in the 8-coordinated (2TMP + $2H_2O$).

The stabilization energies are larger for the Hf case: −74.2 kcal/mol compared to −70.6 kcal/mol for Zr. The stabilization is around 3.6 kcal/mol in favor of Hf, slightly larger than what we observed for the 6-coordinated species. In the case of 2TMP's interacting, it is around 2.7 kcal/mol in favor of Hf, slightly less than the gain in energy in the 6-coordinated case. For comparison, in the lanthanide series, the increase in coordination from 1:1 complex to 1:2 complex in the case of thiophosphoryl ligands, it was found that the size selectivity vanishes and almost similar interaction energies are obtained for La, Eu, and Yb, which was otherwise in the order La > Eu

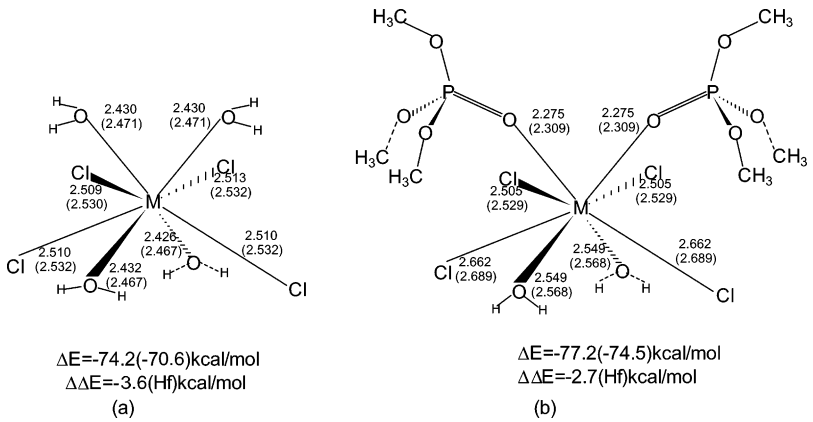

Figure 8. Minimized geometries (Cs symmetry) of MCl_4 interacting with $4H_2O$ (a) and 2TMP + $2H_2O$ (b) molecules. M=Hf/Zr, Zr bond lengths are given in parentheses.

> Yb.[2] Unlike in the lanthanide series, the stoichiometry does not change the trend in Hf and Zr, but reduces the difference to a very small extent (it should be remembered here that Hf^{4+} and Zr^{4+} have nearly the same radius).

Conclusions

Solvent extraction of metal cations and their counterions is a complex procedure involving formation of the complexes (primary interactions) and stabilizations (secondary interactions). Utilizing many experimental observations such as neutrality of the complex, tetravalency, and disolvation we approach the problem of Hf and Zr separation through computational studies. In this study we have used the gas-phase interaction energy of the Hf/Zr complex interacting with the ligands as our model for understanding the extractions and stabilities. We have calculated the relative energies of the stabilization in Hf and Zr complexes at their lowest energy conformations, which turn out to be similar geometries, and thus compared stabilizations of Hf and Zr having equal nonbonded interactions. These studies show that at the molecular level (primary interaction), it is the Hf complex that has larger stability in acetone and TMP solvents, thus indicating that in Hf and Zr solutions which are not complicated by aggregation and polymerization of the metal complexes, Hf would be extracted preferably into the organic solvent. We conclude from this study that the gas-phase interaction energies are sufficient to significantly discriminate Hf and Zr complexes and thus can be used to explain Hf and Zr separation.

Acknowledgment. The authors thank VSSC, Trivandrum for the funding and Dr. K. V. Raghavan, Director, IICT for the constant support. G.G. and S.R. thank VSSC for a fellowship.

References and Notes

(1) (a) Marcus, Y.; Asher, L. E. *J. Phys. Chem*. **1978**, *82*, 1246. (b) Hancock, R. D.; Martell, A. E. *Chem. Rev.* **1989**, *89*, 1875. (c) Horwitz, E. P.; Dietz. M. L.; Fisher, D. E. *Solvent Extr. Ion Exch*. **1990**, *8*, 199. (d) Hay, B. P.; Rustad, J. R. *J. Am. Chem. Soc*. **1994**, *116*, 6316−6326. (e) Dietz, M. L.; Bond, A. H.; Hay, B. P.; Chiarizia, R.; Huber, V. J.; Herlinger, A. W. *Chem. Commun*. **1999**, 1177−1178. (f) Hay, B. P.; Herlinger, A. W.; Bond, A. H.; Chiarizia, R.; Huber, V. J.; Dietz, M. L. *Anal. Chem*. **1999**, *71*, 2757−2765. (g) Nicholas, J. B.; Hay, B. P. *J. Phys. Chem*. **1999**, *100*, 9815−9820. (h) Richard, A. S.; Urvoas, A.; Bryan, J. C.; Haverlock, T. J.; Hay, B. P.; Moyer, B. A. *Chem. Commun.* **1999**, 1751−1752. (i) Bond, A. H.; Dietz, M. L.; Chiarizia, R. **2000**, *39*, 3442−3464. (j) Izatt, N. E.; Bruening, R. L.; Krakowiak, K. E.; Izatt, S. R. *Ind. Eng. Chem. Res*. **2000**, *39*, 3405−3411.

(2) Christian, B.; Wipff, G. *J. Phys. Chem. A* **1999**, *103*, 6023−6029.

(3) Berny, F.; Muzet, N.; Troxler, L.; Dedieu, A.; Wipff, G. *Inorg. Chem*. **1999**, *38*, 1244−1252.

(4) (a) Cosentino, U.; Moro, G.; Pitea, D.; Villa, A.; Carlo, P. F.; Maiocchi, A.; Fulvio, U. *J. Phys. Chem. A* **1998**, *102*, 4606−4614. (b) Nicholas, J. B.; Hay, B. P.; Dixon, D. A. *J. Phys. Chem. A* **1998**. *103*, 1394−1400. (c) Kumph, R. A.; Daugherty, D. A. *Science* **1993**, *261*, 1708−1710. (d) Lhotak, P.; Shinkai, S. *J. Phys. Org. Chem*. **1997**, *10*, 273−285. (e) Mecozzi, S.; West, A. P.; Doueherty, D. A. *J. Am. Chem. Soc*. **1996**, *118*, 2307−2308. (f) Sunner, J.; nishizawa, K.; Kebarle, P. *J. Phys. Chem*. **1981**, *85*, 1814−1820. (g) Hay, B. P.; Dixon, D. A.; Vargas, R.; Garza, J.; Raymond, K. N. *Inorg. Chem*. **2001**, *40*, 3922. (h) Hay, B. P.; Hannock, R. D. *Coord. Chem. Rev*. **2001**, *212*, 61. (i) Hay, B. P.; Firman, T. K. *Inorg. Chem*. **2002**, *41*, 5502. (j) Lumetta, G. J.; Rapko, B. M.; Garza, P. A.; Hay, B. P.; Gilbertson, R. D.; Weakley, J. R.; Hutchison, J. E. *J. Am. Chem. Soc*. **2002**, *124*, 5644.

(5) (a) Wheaton, W, V.; Majumdar, D.; Balasubramanian, K.; Chaue, L.; Allen, P. G. *Chem. Phys. Lett*. **2003**, *371*, 349−359. (b) Majumdar, D.; Roszak, S.; Balasubramanian, K.; Nitsche, H. *Chem. Phys. Lett*. **2003**, *372*, 232−241.

(6) Da silva, A. B. V., Jr.; Distin, P. A. *CIM Bull*. **1998**, *91*, 221−224.

(7) Fischer, W.; Deierling, B.; Heilsch, H.; Otto, G.; Pohlmann, H. P.; Reinhardt, K. *Angew. Chem., Int. Ed. Engl.* **1966**, *5*, 15−23.

(8) Levitt, A. E.; Harry, F. *J. Am. Chem. Soc*. **1956**, *78*, 1545−1549.

(9) El-Ammouri, E.; Distin, P. A. *Solvent Extr. Ion Exch*. **1996**, 871−887.

(10) Suriyachat, D.; Distin, P. A. *Int. Solvent Extr. Conf.* [*Proc.*] **1993**, 265−272.

(11) (a) Golub, A. M.; Sergunkin, V. N. *Zh. Prikil. Khim*. **1970**, *43*, 1203. (b) Sinegribova, O. A.; Yagodin, G. A. *Zh. Neorg. Khim*. **1971**, *16*, 2237.

(12) Frisch, M. J.; Trucks, G. W.; Schlegel, H. B.; Scuseria, G. E.; Robb, M. A.; Cheeseman, J. R.; Zakrzewski, V. G.; Montgomery, J. A.; Stratmann, R. E.; Burant, J. C.; Dapprich, S.; Millam, J. M.; Daniels, A. D.; Kudin, K. N.; Strain, M. C.; Farkas, O.; Tomasi, J.; Barone, V.; Cossi, M.; Cammi, R.; Mennucci, B.; Pomelli, C.; Adamo, C.; Clifford, S.; Octerski, J.; Petersson, G. A.; Ayala, P.; Cui, Q.; Morokuma, M.; Mallik, D. K.; Rabuck, A. D.; Raghavachari, K.; Foresman, J. B.; Cioslowski, J.; Ortiz, J. V.; Stefenov, B. B.; Liu, G.; Liashenko, A.; Piskorz, P.; Komaromi, I.; Gomperts, R.; Martin, R. L.; Fox, D. J.; Keith, T.; Al-Laham, M. A.; Peng, C. Y.; Nanayakkara, A.; Gonzalez, C.; Challacombe, M.; Gill, P. M. W.; Johnson, B.; Chen, W.; Wong, M. W.; Andres, J. L.; Gonzelez, A. C.; Head-Gordon, M.; Peplogle, E. S.; Pople, J. A.; *Gaussian 98*, Revision; Gaussian, Inc.; Pittsburgh, PA. 1998.

(13) (a) te Velde, G.; Bickelhaupt, F. M.; van Gisbergen, S. J. A.; Fonseca Guerra, C.; Baerends, E. J.; Snidjers, J. G.; Ziegler, T. *J. Comput. Chem*. **2001**, *22*, 931−967. (b) Guerra, F. C.; Snidjers, J. G.; te Velde, G.; Baerends, E. *J. Theor. Chem. Acc*. **1998**, *99*, 391. (c) Vrije ADF2002.03, SCM, Theoretical Chemistry, Universiteit, Amsterdam.

(14) Bernardi, N.; Bottoni, A.; Casolari, S.; Tagliavini, E. *J. Org. Chem*. **2000**, *65*, 4783−4790.

(15) Zhou, M.; Chen, M.; Zhang, L. *J. Phys. Chem. A* **2002**, *106*, 9017−9023.

(16) (a) Becke, A. D. *J. Chem. Phys*. **1993**, *98*. 5648. (b) Lee, C.; Yang, W.; Parr, R. G. *Phys. Rev. B* **1998**, *37*, 785.

(17) Dunning, T. H., Jr.; Hay, P. J. In *Modern Theoretical Chemistry*; Schaefer, H. F., III, Ed.; Plenum Press: New York, 1976; Vol. 3, p 1.

(18) Galeffi, B.; Simard, M.; Wuest, J. D. *Inorg. Chem*. **1990**, *29*, 951.

(19) (a) Van Lenthe, E.; Baerends, E. J.; Snijders, J. G. *J. Chem. Phys*. **1993**, *99*, 4597. (b) Van Lenthe, E.; Baerends, E. J.; Snijders, J. G. *J. Chem. Phys*. **1994**, *101*, 9783. (c) Van Lenthe, E.; Baerends, E. J.; Snijders, J. G. *J. Chem. Phys*. **1996**, *105*, 6505−6516. (d) Van Lenthe, E.; Baerends, E. J.; Snijders, J. G. *Int. J. Quantum Chem.* **1996**, 281−293. (e) Van Lenthe, E.; Baerends, E. J. *J. Chem. Phys*. **1999**, *110*, 8943−8953.

(20) (a) Lee, C.; Yang, W.; Parr, R. G. *Phys. Rev. B* **1988**, *37*, 785. (b) Miehlich, B.; Savin, A.; Stoll, H.; Preuss, H. *Chem. Phys. Lett*. **1989**, *157*, 200.

(21) Baerends, E. J.; Ellis, D. E.; Ros, P. *Chem. Phys*. **1973**, *2*, 41.

(22) Boys, S.; Bernardi, F. *Mol. Phys*. **1970**, *19*, 553−566.

(23) Cambridge Crystallographic Database, QUEST 3D Software, X.-Blackboard Version, 2.3.8, 1999.

(24) (a) Duraj, S. A.; Towns, R. L. R.; Baker, J.; Schupp, J. *Acta Crystallogr*. **1990**, *C46*, 890. (b) Eberle, M.; Rohr, C. *Acta Crystallogr*. **1996**, *C52*, 556.

(25) Tse-Lok Ho. *Chem. Rev.* **1975**, *75*, 1−20.

(26) Dobado, J. A.; Uggla, R.; Sundberg, M. R.; Molina, J. *J. Chem. Soc., Dalton Trans*. **1999**, 489−496.

(27) Sato, T. *Solvent Extr. Ion Exch*. **1983**, *1*, 251.